

An Annelated Mesoionic Carbene (MIC) Based Ru(II) Catalyst for Chemo- and Stereoselective Semihydrogenation of Internal and Terminal Alkynes

Suman Yadav, Indranil Dutta, Sayantani Saha, Shubhajit Das, Swapan K. Pati, Joyanta Choudhury, and Jitendra K. Bera*



Cite This: <https://dx.doi.org/10.1021/acs.organomet.0c00413>



Read Online

ACCESS |



Metrics & More

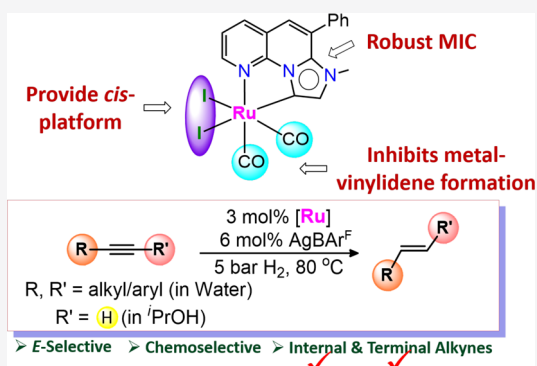


Article Recommendations



Supporting Information

ABSTRACT: The catalytic utility of $[\text{RuL}^1(\text{CO})_2\text{I}_2]$ (**1**), containing an annelated π -conjugated imidazo-naphthyridine-based mesoionic carbene (MIC) ligand (L^1), is evaluated for *E*-selective alkyne semihydrogenation. The precatalyst **1**, in combination with 2 equiv of AgBAR^{F} , semihydrogenates a broad range of internal alkynes with molecular hydrogen (5 bar) in water. (*E*)-Alkenes are accessed in high yields, and a number of reducible functional groups are tolerated. A chelate MIC ligand and two *cis* carbonyls provide a well-defined platform at the Ru center for hydrogenation and isomerization. The loss of two iodides and the presence of two carbonyls render the Ru center electron deficient and thus the formation of metal vinylidenes with terminal alkynes is avoided. This is leveraged for the semihydrogenation of terminal alkynes by the same catalytic system in isopropyl alcohol. Reaction profile, isomerization, kinetic, and DFT studies reveal initial alkyne hydrogenation to a (*Z*)-alkene, which further isomerizes to an (*E*)-alkene via metal-catalyzed *Z* \rightarrow *E* isomerization.

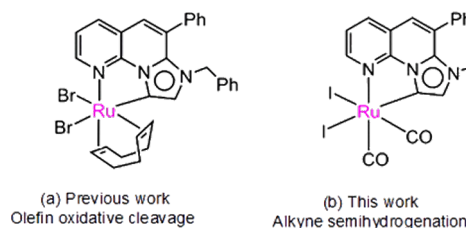


INTRODUCTION

The interest in metal complexes bearing N-heterocyclic carbene (NHC) ligands stems largely from their ability to catalyze a wide variety of organic transformations.¹ A subclass of NHC ligands is mesoionic carbene (MIC), which binds the metal through the imidazole C4 or C5 site instead of C2, giving rise to a stronger σ donation to the metal in comparison to its C2-bound congeners.² Metal NHC catalysts are well suited for oxidation reactions because of their stability under oxidative conditions.³ However, their applications in hydrogenation chemistry are still a considerable challenge.⁴ This is due to the susceptibility of the putative (NHC)metal hydride intermediate toward reductive elimination under the reaction conditions, leading to the breakdown of the catalysts.⁵

An effective approach to suppress ligand dissociation via reductive elimination is to employ chelate ligands.⁶ We previously designed a fused π -conjugated imidazo-naphthyridine system that resembles a MIC analogue of 1,10-phenanthroline. $[\text{Ru}(\text{COD})(\text{MIC})\text{Br}_2]$ (COD = 1,5-cyclo-octadiene) was synthesized, which was found to be an excellent catalyst for the selective oxidative scission of olefins to aldehydes (Scheme 1a).^{3d} Annelation on the ligand construct restricts the rotational flexibility and thus diminishes the prospect of ligand extrusion.⁷ The π delocalization on the ligand architecture offers a higher conjugational stability and enhances the ligand donor capacity in comparison to its

Scheme 1. Annelated MIC Complexes of Ru and Their Catalytic Utilities



nonannelated analogue.⁸ Our interest in hydrogenation chemistry began with the isolation of the Ru complex **1** (Scheme 1b), bearing the related annelated MIC ligand L^1 and two mutually *cis* oriented carbonyls.⁹ A chelate MIC ligand scaffold along with two *cis* CO groups in **1** could provide an ideal platform for hydrogenation and isomerization.

Received: June 16, 2020

Transition-metal-mediated semihydrogenation of alkynes toward stereoselective alkene formation is well documented.¹⁰ A major challenge for alkyne semihydrogenation is the selective formation of an (*E*)-alkene. Most transition-metal catalysts, under either homogeneous¹¹ or heterogeneous¹² conditions, deliver two hydrogen atoms suprafacially to the π -bond of the alkyne, resulting in a *Z*-selective alkene. Because of this intrinsic feature of *Z* selectivity, the synthesis of (*E*)-alkenes is inherently difficult. Conventional methods for the synthesis of (*E*)-alkenes are stoichiometric in nature. A Birch-type reduction of alkynes using alkali metals (Li, Na) is a widely used method for accessing (*E*)-alkenes.¹³ However, low functional group tolerance due to the harsh reaction conditions has been a major drawback. Although some improvement in the scope of selectivity was achieved with the aid of over-stoichiometric amounts of chromium reagents, the use of toxic noncatalytic reagents and the production of copious waste remain significant problems.

Transfer hydrogenation protocols have been employed for alkyne to alkene conversions.¹⁴ In 1999, Tani and co-workers used methanol as the hydrogen source for *trans*-alkene synthesis catalyzed by an Ir complex.¹⁵ Trost et al. developed a two-stage *trans*-hydrosilylation/proto-desilylation pathway for alkyne reduction to (*E*)-alkenes.¹⁶ Selective *E* configurations were also achieved by using organic or inorganic acids in the form of hydrogen sources via a transfer hydrogenation methodology.¹⁷ Liu and Luo reported ligand-controlled CO-PNP catalysts for semihydrogenation of alkynes to (*Z*)- and (*E*)-alkenes using ammonia–borane.¹⁸ Yang and Sun showed ligand-controlled selectivity to access (*E*)- and (*Z*)-alkenes with EtOH as the hydrogen source using an Ir catalyst.¹⁹ Recently, Kann and co-workers have employed alcohols as hydrogen donors with 1 equiv of ^tBuOK to hydrogenate alkynes with a Ru catalyst.²⁰ Although these transfer hydrogenation methodologies are superior alternatives to Birch reduction in terms of functional group compatibility, they invariably produce stoichiometric amounts of waste. Bargon²¹ and Fürstner²² demonstrated ruthenium-catalyzed direct *E* hydrogenation using molecular H₂. Milstein,²³ Fout,²⁴ and Beller²⁵ have reported base-metal catalytic systems for accessing (*E*)-alkenes under a hydrogen atmosphere. Bimetallic complexes have also been reported for catalytic hydrogenation of alkynes with molecular hydrogen.²⁶ A major limitation that persists in the homogeneous catalytic alkyne hydrogenation with molecular hydrogen is that most of the catalysts are ineffective for terminal alkynes possibly due to the formation of a stable metal vinylidene complex or catalyst decomposition under the reaction conditions.²⁷

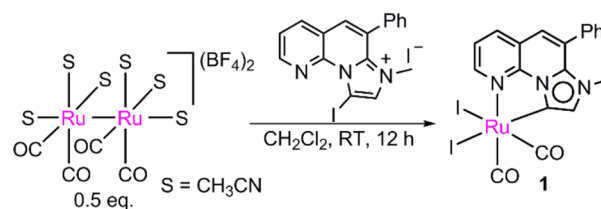
Herein we report the catalytic utility of complex **1** for semihydrogenation of both internal and terminal alkynes. We reasoned that the removal of two iodo ligands from the metal would give rise to a dicationic complex with diminished electron density on the metal center. The presence of two CO groups would further boost the metal electrophilicity. The electron deficiency at the ruthenium is likely to make the catalyst reluctant toward the formation of a metal vinylidene with terminal alkynes. Thus, catalyst **1** efficiently hydrogenates internal and terminal alkynes to their corresponding alkenes.

RESULTS AND DISCUSSION

Catalytic Studies. Complex **1** was synthesized following a procedure reported previously.⁹ The reaction of [L¹]I with [Ru₂(CH₃CN)₆(CO)₄][BF₄]₂ in a 2:1 molar ratio in CH₂Cl₂

at room temperature afforded the neutral complex [Ru(L¹)(CO)₂I]₂ (**1**) as an orange solid in 82% yield (Scheme 2). The

Scheme 2. Synthesis of **1**



molecular structure reveals an annelated MIC ligand that chelates the Ru center through the carbene carbon and the naphthylidene nitrogen. Two mutually *cis* oriented carbonyls and two iodides occupy the remaining sites to complete an octahedral geometry around the metal center.

The catalytic utility of **1** was evaluated for the semihydrogenation of internal and terminal alkynes. AgBAR^F was employed to create vacant sites at the metal center by the removal of the iodides. The initial reaction of diphenylacetylene (0.2 mmol), catalyst **1** (5 mol %), and AgBAR^F (10 mol %) in dry isopropyl alcohol in the presence of 5 bar of H₂ pressure at 80 °C afforded full conversion of the alkyne to (*E*)-stilbene and 1,2-diphenylethane in a 92:8 ratio after 4 h (entry 1, Table S1). Using water as a solvent, 92% conversion was observed for the model reaction with a 90:10 *E*:*Z* ratio (entry 2). When the reaction time was increased from 4 to 7 h, 98% of the alkyne was converted with an excellent *E* selectivity (entry 3). Acetonitrile, toluene, dioxane, tetrahydrofuran, methanol, and ethanol were proved to be inefficient in terms of yield and selectivity (entries 4–9). Further, reduction of diphenylacetylene was carried out in water with various additives, such as, KBAR^F, AgOTf, AgSbF₆, AgBF₄, AgPF₆, KPF₆, NH₄PF₆, and TIPF₆ (entries 10–17). A maximum 35% conversion was achieved with poor selectivity. In the absence of any additive, only 12% conversion was achieved after 12 h (entry 18). Reducing the catalyst loading from 5 to 3 mol % did not amend the conversion and selectivity for the model reaction (entry 19). Further reduction of the catalyst loading diminished the rate of the reaction and the selectivity as well. Decreasing the H₂ pressure from 5 to 4 bar resulted in a lower conversion of the diphenylacetylene. The reaction temperature has a critical effect on this reaction. An abrupt decrease in the reaction rate was observed when the reaction was carried out at an elevated temperature (>90 °C).

Under the optimized reaction conditions (alkyne/pH₂/catalyst/AgBAR^F = 0.2 mmol/5 bar/3 mol %/6 mol % in 4 mL of H₂O at 80 °C), a variety of internal alkynes were subjected to semihydrogenation catalyzed by **1**, and the results are summarized in Table 1. Diphenylacetylene and its electron-rich derivatives 1,2-di-*p*-tolylethyne and 1-methoxy-4-(phenylethynyl)benzene afforded the corresponding (*E*)-alkene products in excellent yields (90–94%) and selectivity (97:3 to 99:1, *E*:*Z*) (entries 1–3). An amino-group-substituted internal alkyne showed a slightly lower yield of 81% (entry 4). The semihydrogenation of 4-(phenylethynyl)benzaldehyde gave an 88% yield with good *E* selectivity (93:7, *E*:*Z*) after 9 h (entry 5). Internal alkynes bearing electron-withdrawing keto and ester groups on the para position afforded the corresponding (*E*)-alkenes (86% and 82% yields, respectively, entries 6 and 7) with good selectivity (90:10, *E*:*Z*). 4-

Table 1. Semihydrogenation of Internal Alkynes^a

Entry	Major product	Time (h)	Yield (%) ^b	E/Z/Alkane ^c
1		7	90	98:2:0
2		7	92	99:1:0
3		7	94	97:3:0
4		7	81	95:5:0
5		9	88	93:7:0
6		9	86	90:10:0
7		9	82	90:10:0
8		9	80	89:11:0
9		9	65	70:30:0
10		9	60	65:0:35
11		4	96	98:0:2
12		4	93	95:0:5
13		4	87	90:0:10
14 ^d		5	94	99:1:0
15		2	96	99:1:0
16		2	96	99:1:0

^aReaction conditions unless specified otherwise: alkynes (0.2 mmol), catalyst (3 mol %), AgBARF (6 mol %), 80 °C, H₂O (4 mL), 5 bar of H₂. ^bIsolated yield. ^cDetermined by GC-MS analysis. ^dReaction in ^tPrOH.

(Phenylethynyl)benzonitrile gave the semireduced alkene product with 80% yield with high selectivity (89:11, *E*:*Z*) (entry 8). These observations clearly show that the nitrile, ester, aldehyde, and ketones are well tolerated under the mild reaction conditions. The poor selectivity observed for internal alkynes having hydroxy and pyridine groups are accounted for by its coordination to the metal center (entries 9 and 10). A significant amount of alkane also formed in the case of pyridine containing an internal alkyne. The hydrogenation of internal alkynes with a carbonyl functionality directly attached to the acetylenic carbon was also investigated. These substrates are completely converted to their corresponding alkenes within 4 h with high *E* selectivity. 4-Phenyl-3-butyne-2-one and 1,3-diphenyl-2-propyn-1-one afforded 96% and 93% of the

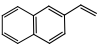
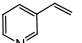
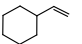
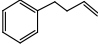
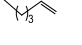
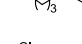
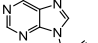
corresponding (*E*)-alkene products, respectively (entries 11 and 12). Methyl phenylpropiolate resulted in 87% of the corresponding (*E*)-alkene (entry 13). An internal alkyne containing a trimethylsilyl (TMS) group gave acetophenone under the reaction conditions. However, using ^tPrOH as solvent, an excellent yield of 94% with high selectivity (99:1, *E*:*Z*) was obtained after 5 h (entry 14). Internal alkynes bearing an aliphatic group such as aryl alkyl and dialkyl substituted acetylenes were also converted to their desired alkene products with an excellent yield of 96% and selectivity of 99:1 (*E*:*Z*) (entries 15 and 16).

Semihydrogenation of terminal alkynes is challenging due to the propensity to form a stable vinylidene complex with the catalyst.²⁷ Bargon²¹ and Fürstner²² noted that the Ru-based catalysts form the corresponding metal vinylidene complexes and become inactive for terminal alkynes. Removal of two iodo ligands from the metal and the presence of two carbonyls may make the metal center sufficiently electron deficient to prevent the formation of the metal vinylidene with terminal alkynes. This exciting possibility for the catalyst **1** prompted us to explore semihydrogenation of the terminal alkynes. The reaction was performed under the optimized conditions using ^tPrOH as a solvent instead of water, since terminal alkynes give the alkyne hydration product ketones in the presence of silver salts and water.²⁸ The results are summarized in Table 2. Phenylacetylene and its electron-donating derivatives such as 4-methyl-, 3-methyl-, and 4-methoxyphenylacetylene gave full conversions with an excellent selectivity of up to 99:1 (alkene:alkane) within 2 h (entries 1–4). Electron-withdrawing groups on the aromatic ring such as 4-acetoxy- and 4-cyanophenylacetylene afforded 88% and 83% yields, respectively, with 99:1 alkene:alkane ratio (entries 5 and 6). 4-Fluoro- and 2-fluorophenylacetylenes were converted to their corresponding alkenes in 79% (96:4, alkene:alkane) and 76% yields (98:2, alkene:alkane), respectively, after 4 h (entries 7 and 8). 4-Chloro- and 4-bromophenylacetylene gave 83% and 86% yields, respectively, with a 98:2 alkene:alkane ratio (entries 9 and 10). 2-Ethynyl-naphthalene afforded a 94% yield of the corresponding terminal alkene (entry 11). The heterocyclic alkyne 3-ethynylpyridine gave a 63% yield in 2 h with an 85:15 alkene:alkane ratio (entry 12). Using ethynylcyclohexyl as a substrate, an 89% yield was observed in 1 h with a product ratio of alkene to over-reduced alkane of 99:1 (entry 13). The same protocol was extended for aliphatic terminal alkynes. Long-chain aliphatic alkynes showed excellent yields and selectivity. 4-Phenyl-1-butyne gave 4-phenyl-1-butene in 90% yield (entry 14). Reduction of 1-hexyne and 4-pentyn-1-ol afforded the corresponding terminal alkenes with 85% and 82% yields, respectively, in 1 h (entries 15 and 16). Continuing the reaction for a longer time increases the over-reduced alkane product. Semihydrogenation of alkyne appended to a purine base gave the corresponding alkene in 92% yield (entry 17).

A comparison of the catalytic performances of a select set of reported catalysts (Figure S4) reveals the catalytic efficacy of **1** toward the semihydrogenation of terminal alkynes.

Reaction Profile. To gain mechanistic insight, the reaction profile was monitored using diphenylacetylene as the model substrate (Figure 1). Initially, (*Z*)-stilbene is formed and reaches a maximum (~50%) at 110 min. Then onward it slowly isomerizes to (*E*)-stilbene and is finally consumed completely at 300 min. Although (*E*)-stilbene appears at the initial stage of the reaction, its growth is improved rapidly at

Table 2. Semihydrogenation of Terminal Alkynes^a

$\text{R}-\text{C}\equiv\text{C}-\text{H} \xrightarrow[\text{H}_2 (5 \text{ bar}), \text{}^i\text{PrOH} (4 \text{ mL}), 80^\circ\text{C}]{\text{1 (3 mol\%)}, \text{AgBAR}^{\text{F}} (6 \text{ mol\%})} \text{R}-\text{CH}=\text{CH}_2 + \text{R}-\text{CH}_2-\text{CH}_3$				
Entry	Major product	Time (h)	Yield (%) ^b	Alkene/Alkane ^c
1	R = H	2	90	97:3
2	R = 4-CH ₃	2	91	98:2
3	R = 3-CH ₃	2	90	98:2
4	R = 4-OCH ₃	2	94	99:1
5	R = 4-COOCH ₃	4	88	99:1
6	R = 4-CN	4	83	99:1
7	R = 4-F	4	79	96:4
8	R = 2-F	4	76	98:2
9	R = 4-Cl	4	83	98:2
10	R = 4-Br	4	86	98:2
11		4	94	99:1
12		2	63	85:15
13		1	89	99:1
14		1	90	99:1
15		1	85	99:1
16		1	82	99:1
17		3.5	92	99:1

^aReaction conditions: alkynes (0.2 mmol), catalyst (3 mol %) AgBAR^F (6 mol %), 80 °C, ⁱPrOH (4 mL), 5 bar of H₂. ^bIsolated yield.

^cDetermined by GC-MS analysis.

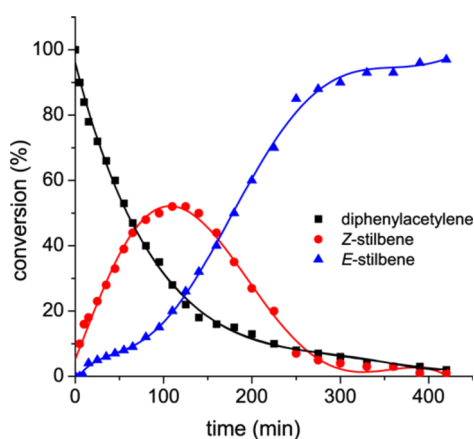


Figure 1. Reaction profile for alkyne semihydrogenation.

around 110 min, finally reaching a maximum plateau after 300 min. The decreasing alkyne concentration leads to an increase in the rate of alkene isomerization process. The isomerization

process is inhibited by the alkyne at a higher concentration due to the greater affinity of diphenylacetylene for **1** in comparison to (Z)-stilbene.

cis–trans Isomerization Study. The reaction profile indicates that the alkyne is initially reduced to (Z)-stilbene, which is then isomerized to (E)-stilbene under the reaction conditions. To investigate the Z to E isomerization, a series of controlled reactions was carried out. Under the optimized reaction conditions, (Z)-stilbene is completely converted to the thermodynamically stable (E)-stilbene with a trace amount of alkane (entry 1, Table 3). However, when (E)-stilbene was

Table 3. Alkene Isomerization Study^a

$\text{Ph}-\text{CH}=\text{CH}-\text{Ph} \xrightarrow[\text{H}_2 (5 \text{ bar}), \text{H}_2\text{O} (4 \text{ mL}), 80^\circ\text{C}, 7 \text{ h}]{\text{1 (3 mol\%)}, \text{AgBAR}^{\text{F}} (6 \text{ mol\%})} \text{Ph}-\text{CH}=\text{CH}-\text{Ph} + \text{Ph}-\text{CH}=\text{CH}-\text{Ph} + \text{Ph}-\text{CH}_2-\text{CH}_2-\text{Ph}$			
entry	alkene	reaction conditions	E:Z:alkane ^b
1	(Z)-stilbene	same	96:0:4
2	(E)-stilbene	same	98:0:2
3	(Z)-stilbene	no catalyst	40:60:0
4	(Z)-stilbene	no H ₂	<1:99:0

^aReaction conditions: alkynes (0.2 mmol), catalyst (3 mol %), AgBAR^F (6 mol %), 80 °C, H₂O (4 mL), 5 bar of H₂. ^bProduct ratio was determined by GC-MS analysis (Figures S5–S8 in the Supporting Information) using mesitylene as an internal standard.

employed, no isomerization was observed (entry 2). Carrying out a reaction with (Z)-stilbene in the absence of the catalyst led to 40% isomerized product (entry 3). The isomerization process did not occur when the reaction was conducted in the absence of H₂ (entry 4). It can thus be concluded that (Z)-stilbene is a feasible kinetic intermediate that isomerizes into the thermodynamically stable (E)-stilbene under the reaction conditions. The *cis–trans* isomerization is accelerated by a H₂-derived metal hydride species that is consistent with the observation by Mankad^{26a} and Fout.²² Liu and Luo also emphasized the role of ammonia–borane for the isomerization process by a cobalt catalyst.¹⁸

Kinetic Studies. The initial rate of the reaction was monitored (up to <10–15% conversion) to determine the reaction order with respect to catalyst **1**, alkyne (diphenylacetylene), and hydrogen. To find out the order with respect to H₂ pressure, the concentrations of diphenylacetylene and catalyst **1** were kept constant and the H₂ pressure was varied between 0 and 40 bar. The reaction rate increased with increasing H₂ pressure. A plot of ln[rate] vs ln[pH₂] yielded a linear dependence with a slope value of ~1.0 (Figure 2a). It reveals the first-order dependence of the reaction rate with respect to hydrogen and thus indicates the involvement of one molecule of hydrogen in one of the slow steps of the catalytic cycle. With respect to the substrate, the concentration of diphenylacetylene was varied, with H₂ pressure and catalyst concentration kept constant, which led to an increased rate of the reaction with increasing substrate concentration. A plot of ln[rate] vs ln[substrate] resulted in a straight line with a slope of 0.56 (Figure 2b). To derive the order with respect to the catalyst, its amount was varied, with the concentration of substrate and hydrogen pressure kept constant. With increasing catalyst concentration, the rate of the reaction also increased. A plot of ln[rate] vs ln[catalyst] showed a straight line with a slope value of 0.46 (Figure 2c). Hence, the experimental rate law for the reaction is

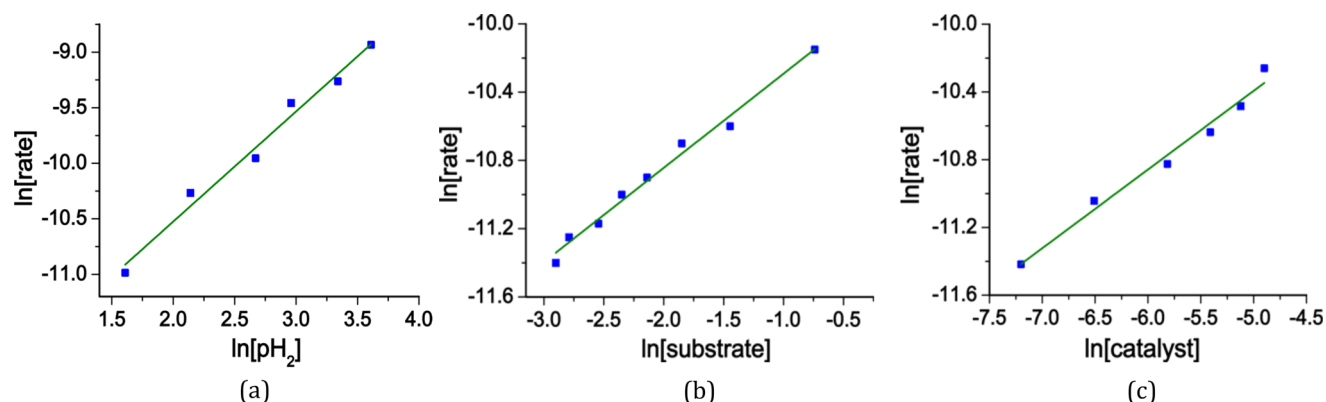


Figure 2. Plot of $\ln[\text{rate}]$ vs $\ln[\text{pH}_2]$ (a), $\ln[\text{substrate}]$ (b), and $\ln[\text{catalyst}]$ (c).

$$\text{rate} = k_{\text{obs}}[\text{catalyst}]^{0.5}[\text{alkyne}]^{0.5}[\text{H}_2]^1 \quad (1)$$

Eyring Plot. The effect of temperature on the rate of diphenylacetylene semihydrogenation catalyzed by **1** was also examined. An Eyring plot of $\ln(k/T)$ versus $1/T$ in the temperature range 323–358 K was used to determine the activation parameters (Figure 3). The estimated entropy of

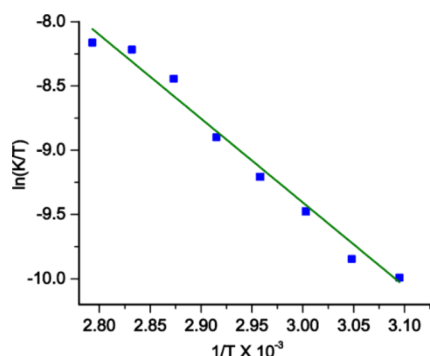


Figure 3. Eyring plot for semihydrogenation of diphenylacetylene with catalyst **1**.

activation (ΔS^\ddagger) is $-26.95 \pm 1.88 \text{ cal mol}^{-1} \text{ K}^{-1}$, and the enthalpy of activation (ΔH^\ddagger) is $12.9 \pm 0.64 \text{ kcal mol}^{-1}$. A large negative value of ΔS^\ddagger is indicative of an ordered transition state and also supports an associative pathway for the reaction.

Hammett Plot. The initial rates of the reactions of electronically varied para-substituted diphenylacetylene ($p\text{-YPhC}\equiv\text{CPh}$; $\text{Y} = \text{OMe}, \text{Me}, \text{H}, \text{COCH}_3, \text{COOCH}_3$) with “**1** + AgBAR^F ” were measured. The Hammett plot of $\log[\text{initial rate}]$ vs σ (Hammett constant) resulted in a straight line with a ρ value of -0.34 (Figure 4). A negative ρ value suggests that the electron-donating substituents should accelerate the rate of the reaction. However, when $\log[\text{initial rate}]$ was plotted against standard σ^+ values, linearity could not be obtained. These observations indicate that the turnover-limiting transition state of the reaction has partial positive charge deployment over the entire system, which points to a concerted mechanism.

Proposed Mechanism. Reaction profile, isomerization, and kinetic studies suggest the initial formation of a (*Z*)-alkene which subsequently isomerizes to the *E* isomer under the catalytic conditions. Accordingly, a plausible mechanism is proposed which consists of two sequential catalytic cycles (Figure 5). The active catalyst is likely to be **A**, which is

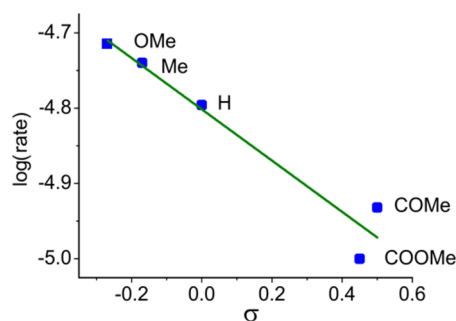


Figure 4. Hammett plot for the competitive hydrogenation of diphenylacetylene and para-substituted derivatives catalyzed by catalyst **1**.

derived from **1** and was characterized spectroscopically. A solution of **1** and AgBAR^F in CH_3CN was stirred at room temperature for 30 min, resulting in a yellow precipitate of AgI . The reddish solution was filtered off and then subjected to ESI-MS analysis. A signal at m/z 250.5377 ($z = 2$) corresponds to the $[\text{Ru}(\text{L}^1)(\text{CO})_2(\text{CH}_3\text{CN})_2]^{2+}$ unit (Figure S12). IR spectral analysis of the same solution showed a shift in carbonyl stretching frequencies to 2020 and 2082 cm^{-1} from the corresponding values 1986 and 2062 cm^{-1} in **1** (Figure S13).²⁹ This is consistent with a significant reduction in electron density at the metal center caused by the removal of two iodides and further augmented by two carbonyls.

In the next step, alkyne becomes bound to the metal to generate the active catalyst **B**. From kinetic experiments, we observed a half-order dependency with respect to the catalyst that prompted us to invoke the off-cycle dimeric species **C**, which is in equilibrium with the catalytically active monomer **B**.³⁰ It is pertinent to note here that alkyne-bridged binuclear ruthenium and rhodium complexes have been proposed as potential intermediates for the hydrogenation of alkynes to (*E*)-alkenes.^{31,21} The proposed alkyne-bridged dimer **C**, prior to the resumption of the catalytic cycle, also accounts for the half-order dependence on alkyne. The derived rate equation (see the Supporting Information) is consistent with the observed rate law (eq 1). A fractional order reaction with respect to alkyne, as discussed by Elsevier and co-workers, suggests that the substrate is involved in an equilibrium that precedes the rate-determining step.³² The subsequent reaction of **B** with H_2 leads to the formation of metal-bound dihydrogen intermediate **D**.^{21,22} To avoid coordinative over-saturation at the metal center by H_2 oxidative addition, we opted for a concerted oxidative hydrogen migration in species

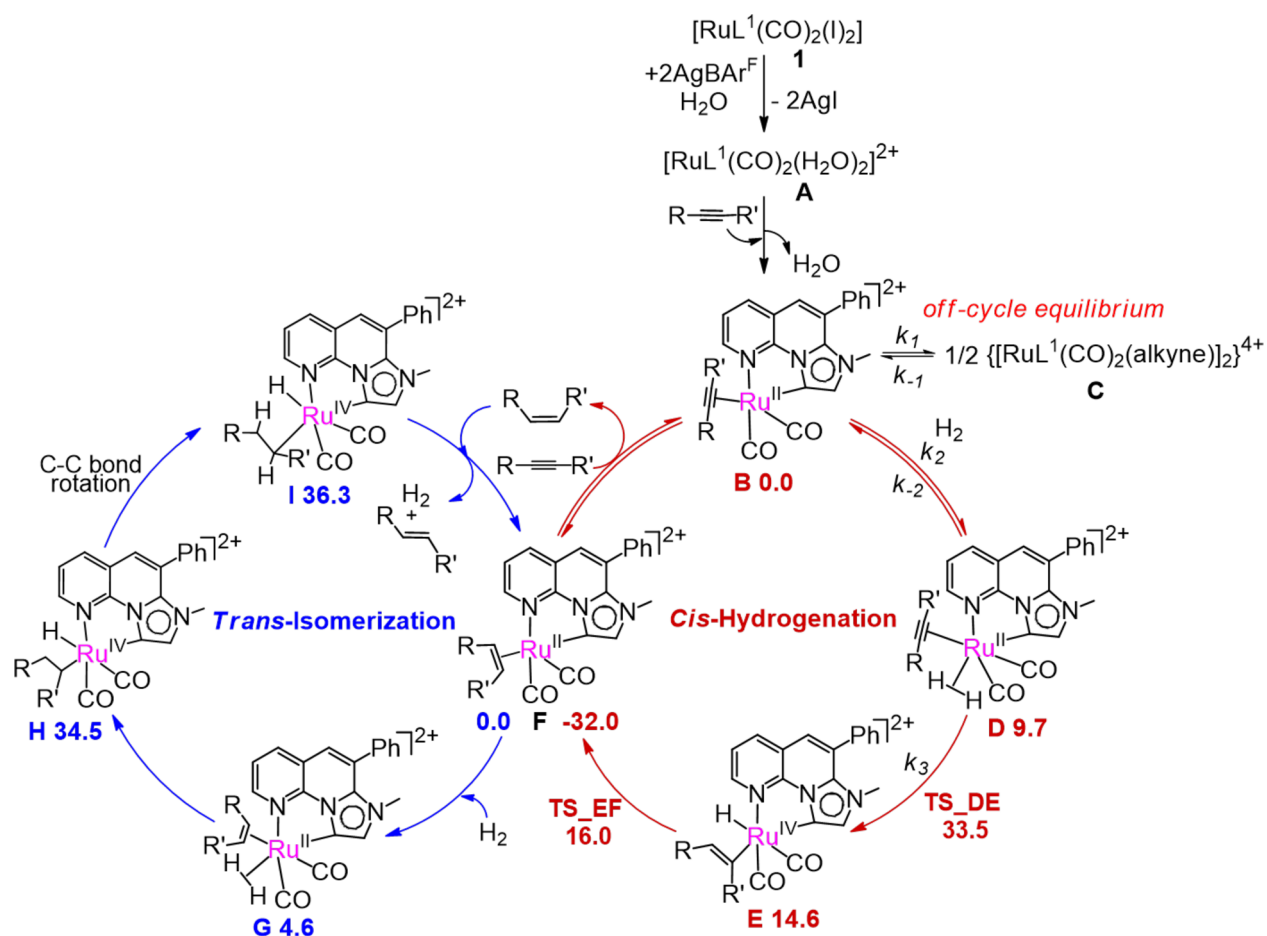


Figure 5. Proposed mechanism of alkyne semihydrogenation. Dimethylacetylene is used as the model substrate for DFT calculations. The free energy of F is set as 0 for the isomerization cycle. Energy values are given in kcal mol⁻¹.

D to the metal-coordinated alkyne, leading to the formation of the metal hydride intermediate E. A similar oxidative hydrogen migration was reported for the hydrogenation of styrene with the cationic ruthenium(II) pyridyl(benzoxazole) system.³³ The development of partial positive charge on the transition state evident from the Hammett studies and a large negative ΔS^\ddagger value obtained from the Eyring plot support such a concerted oxidative hydrogen migration as the rate-determining step of the reaction. The catalytic cycle is closed after the release of the (*Z*)-alkene via reductive elimination from the Ru center, and alkyne readily occupies the vacant site to regenerate B.

The second catalytic cycle begins with the coordination of an H_2 molecule to the metal center in F, leading to the formation of G. A similar hydride migration to metal-bound alkene leads to the formation of intermediate H, a Ru(IV) species which leads to the intermediate I via carbon–carbon bond rotation. Subsequent β -hydride elimination with concomitant release of (*E*)-stilbene closes the cycle with regeneration of the intermediate F. Similar (*Z*)- to (*E*)-alkene isomerization has been reported by Fout²⁴ and Beller.²⁵ A competitive reductive elimination of the alkane product from intermediate I is also possible, though it is likely to be a kinetically slower process in comparison to a β -hydride elimination. Detailed DFT studies from the Beller group have shown that the barrier for a competitive reductive elimination path for alkane formation is 6 kcal mol⁻¹ higher in comparison to the β -hydride elimination.²⁵ Overall, the

proposed mechanistic cycles correlate well with the experimental findings.

DFT computations were carried out with the M06 functional (full computational details are provided in the Experimental Section) to support the experimentally proposed mechanism using dimethylacetylene as the model substrate.³⁴ The Gibbs free energy values for all computed intermediate/transition state (TS) structures are displayed in Figure 5, and all optimized geometries are provided in Figures S14–S16 in the Supporting Information. A monomeric η^2 -alkyne-bound pentacoordinated Ru species, B, is used as the entry point to the *cis*-hydrogenation cycle. Upon coordination of a hydrogen molecule, B transforms into D in an endergonic reaction step. The oxidative hydrogen migration to the alkyne moiety occurs through TS_{DE}, which lies at 33.5 kcal mol⁻¹. The reductive elimination from E has a rather low free energy barrier, leading to the intermediate, F. TS_{EF} lies only 1.4 kcal mol⁻¹ above E. The E to F transformation is highly exergonic and the overall *cis*-hydrogenation process is thermodynamically favored by 32.0 kcal mol⁻¹. F corresponds to (one of) the resting state(s) of the reaction. This justifies the lag between the *cis*-hydrogenation and isomerization processes, as observed during the kinetic analysis of the reaction profile. The overall free energy activation barrier for the *cis*-hydrogenation cycle corresponds to TS_{DE} and it is consistent with the observed reactivity at the experimental temperature. The subsequent isomerization cycle begins with F as the entry point. First, an H_2 molecule coordinates to F to yield G, which converts to H

after oxidative insertion of the hydride in an endergonic reaction step. After the rotation of the C–C bond in **H**, **I** is formed in a marginally endergonic step. A β -hydride elimination followed by the expulsion of the H_2 returns back **F** for resumption of the catalytic cycle. The β -hydride elimination proceeds with a low energy barrier with **TS_{βhe}** lying only 1.2 kcal mol^{−1} above **I**. Overall, our computational results are in line with the experimental observations.

CONCLUSIONS

An annelated chelate MIC and two *cis* carbonyls at the Ru sets up a platform for alkyne semihydrogenation and subsequent *Z* → *E* isomerization. The catalytic system **1**/BAR^F displays broad substrate scope and excellent functional group tolerance to afford (*E*)-alkenes from internal alkynes and molecular hydrogen in water. The catalyst is further distinguished by its ability to semihydrogenate terminal alkynes to the corresponding alkenes in isopropyl alcohol. Reaction profile and isomerization studies confirm the initial formation of (*Z*)-alkenes and subsequent metal-catalyzed isomerization to the *E* products. A two-cycle mechanism, a reduction cycle and an isomerization cycle, is proposed on the basis of experimental results and also supported by DFT calculations. This work further underlines the general utility of the annelated π -conjugated carbene ligand for hydrogenation chemistry.

EXPERIMENTAL SECTION

General Procedures. All reactions with metal complexes were carried out under an atmosphere of purified nitrogen using standard Schlenk-vessel and vacuum-line techniques. Glassware was flame-dried under vacuum prior to use. ¹H NMR spectra were obtained on JEOL JNM-LA 400 and 500 MHz spectrometers. ¹H NMR chemical shifts were referenced to the residual hydrogen signal of the deuterated solvents. The chemical shift is given as a dimensionless δ value and is frequency-referenced relative to TMS for ¹H and ¹³C NMR spectroscopy. GC-MS experiments were performed on an Agilent 7890A GC and 5975C MS system. Hydrogenation reactions were performed at constant pressures using a stainless steel 25 mL Parr hydrogenation reactor. ESI-MS measurements were recorded on a Waters Micromass Quattro Micro triple-quadrupole mass spectrometer. Infrared spectra were recorded on a Bruker Vertex 70 FTIR spectrophotometer in the range 400–4000 cm^{−1}. Elemental analyses were performed on a Thermoquest EA1110CHNS/O analyzer. The crystallized compound was washed several times with dry diethyl ether, powdered, and dried under vacuum for at least 48 h prior to elemental analyses. TLC analyses were performed on commercial TLC paper, and silica gel (100–200 mesh) was used for column chromatography.

Materials. Solvents were dried by conventional methods, distilled under nitrogen, and deoxygenated prior to use. RuCl₃·*x*H₂O was purchased from Arora Matthey, India. All other chemicals were purchased from Sigma–Aldrich. The ligand [L¹I],⁹ [Ru₂(CH₃CN)₆(CO)₄][BF₄]₂,³⁵ and AgBAR^{F36} were prepared according to literature procedures.

Synthesis and Characterization of 1. The synthesis of complex **1** were reported previously by us.⁹ A dichloromethane solution (10 mL) of [L¹I] (56 mg, 0.11 mmol) was added dropwise to a dichloromethane solution (15 mL) of [Ru₂(CO)₄(CH₃CN)₆][BF₄]₂ (40 mg, 0.054 mmol), and the solution was stirred for 12 h at room temperature. A bright yellow solution appears during the reaction. After completion of the reaction dichloromethane was evaporated and the residue was washed with diethyl ether and dried under vacuum. X-ray-quality crystals were grown again, and the cell parameters match those of the earlier report. Yield: 52 mg (82%). ¹H NMR (500 MHz, CD₃CN, 294 K): δ 9.01 (d, *J* = 4.6 Hz, 1H), 8.54 (d, *J* = 8 Hz, 1H), 8.11 (s, 1H), 7.93 (s, 1H), 7.87 (m, 1H), 7.59 (m, 3H), 7.49 (d, *J* =

6.9 Hz, 2H), 3.39 (s, 3H), ¹³C NMR (125 MHz, CD₃CN, 294 K): 195.3, 187.4, 178.5, 150.1, 142.9, 140.1 138.8, 136.2, 135.3, 133.3, 130.1, 129.8, 129, 125.9, 124.9, 124.7, 118.9, 29.4. Anal. Calcd for (C₁₉H₁₃I₂N₃O₂Ru)(CH₃CN)_{0.5}: C, 34.61; H, 2.39; N, 7.07. Found: C, 33.49; H, 2.28; N, 7.26. ESI-MS, *m/z*: 543.9171 [RuL¹(CO)₂I]⁺.

General Procedure for the Semihydrogenation of Internal Alkynes. A cleaned and predried autoclave was charged with the calculated amount of alkyne derivative (0.2 mmol), catalyst (0.006 mmol), and AgBAR^F (0.012 mmol) in 4 mL of deionized water. The autoclave was then pressurized with H₂ (5 bar), and the mixture was stirred at 80 °C. After 2–9 h, the autoclave was cooled and the hydrogen pressure was released carefully. The reaction mixture was extracted with EtOAc (5 mL), and the extract was passed through a short column of silica gel and subjected to GC-MS analysis. To characterize the alkene via NMR spectroscopy, after completion, the reaction mixture was extracted with EtOAc (3 × 10 mL). The combined extracts were dried over Na₂SO₄ and concentrated under vacuum, and the residue was purified by column chromatography using silica gel (hexane/EtOAc 10/0 → 9/1) to afford the alkene.

General Procedure for the Semihydrogenation of Terminal Alkynes. An identical procedure was followed for the semihydrogenation of terminal alkynes, using the calculated amount of alkyne derivative (0.2 mmol), catalyst (0.006 mmol), and AgBAR^F (0.012 mmol) in 4 mL of ³PrOH. After 1–4 h, the reaction mixture was diluted with EtOAc (5 mL), passed through a short column of silica gel, and subjected to GC-MS analysis. To characterize the alkene via NMR spectroscopy, after completion, the reaction mixture was dried under vacuum and the residue was purified by column chromatography using silica gel (hexane/EtOAc 10/0 → 9/1).

General Procedure to Obtain Reaction Profile. A cleaned and predried autoclave was charged with the calculated amount of diphenylacetylene (0.1 mmol), catalyst (0.003 mmol), AgBAR^F (0.006 mmol), and mesitylene (0.1 mmol) in 2 mL of deionized water. The autoclave was then pressurized with H₂ (5 bar) and the mixture was stirred at 80 °C. After 5 min, the autoclave was cooled and the hydrogen pressure was released carefully. The reaction mixture was extracted with EtOAc (5 mL), passed through a short column of silica gel, and subjected to GC-MS analysis. The same methodology was repeated to find out the conversion at different time intervals.

General Procedure for Alkene Isomerization Study. A cleaned and predried autoclave was charged with the calculated amount of *cis* or *trans*-stilbene (0.1 mmol), catalyst (0.003 mmol), AgBAR^F (0.006 mmol), and mesitylene (0.1 mmol), in 2 mL deionized water. The autoclave was then pressurized with H₂ (5 bar), and the mixture was stirred at 80 °C. After 7 h, the autoclave was cooled and the hydrogen pressure was released carefully. The reaction mixture was extracted with EtOAc (5 mL), and the extract was passed through a short column of silica gel and subjected to GC-MS analysis.

Computational Details. All molecular geometries were fully optimized in water (in accordance with the experiments) with the M06³⁴ functional using the 6-31+g(d,p) basis set for lighter atoms and the LANL2DZ basis set along with the corresponding pseudopotential for the Ru atom. Solvent effects (water) were considered within the framework of the SMD model by Truhlar and Cramer.³⁷ All geometry optimizations were followed by a harmonic vibrational analysis to characterize the nature of the stationary points: transition states (one imaginary frequency) or minima (no imaginary frequencies). Intrinsic reaction coordinate (IRC) calculations were performed to verify the transition states. The computed enthalpies and Gibbs free energy values include zero-point energy and thermal corrections at 353.15 K and 1 atm pressure. The thermochemical corrections were obtained within the quasi-harmonic approximation by Cramer and Truhlar, in which all vibrational frequencies below 100 cm^{−1} were raised to 100 cm^{−1}.³⁸ All Gibbs free energy data reported in the manuscript were computed at the SMD(water)/M06/{6-31+G(d,p)+(LANL2DZ+ECP)} level of theory. All calculations were performed using the Gaussian 16 suite of programs.³⁹

■ ASSOCIATED CONTENT

SI Supporting Information

The Supporting Information is available free of charge on the ACS Publications Web site. The Supporting Information is available free of charge at <https://pubs.acs.org/doi/10.1021/acs.organomet.0c00413>.

¹H and ¹³C NMR spectra of **1**, ESI-MS spectrum of **1**, select catalysts for *E*-selective alkyne semihydrogenation, optimization table for semihydrogenation, general procedure for kinetic studies and data, plots of initial rates vs H₂ of and ln[rate] vs ln[H₂], plots of initial rate vs substrate and of ln[rate] vs ln[substrate], plots of initial rate vs catalyst and of ln[rate] vs ln[catalyst], Eyring plot, kinetic rate equation for alkyne semihydrogenation, ESI-MS spectrum of [Ru(L¹)-(CO)₂(CH₃CN)₂]²⁺, IR spectra of **1** and [Ru(L¹)-(CO)₂(CH₃CN)₂]²⁺, optimized structures of intermediates and TSs for the hydrogenation cycle, optimized structures of intermediates for the isomerization cycle, optimized structures of TS_{βhe} and TS_{rea}, energy profile for the hydrogenation cycle, NMR spectra, and GC-MS spectra of selected compounds from Table 1 (PDF)

Cartesian coordinates of the calculated structures (XYZ)

■ AUTHOR INFORMATION

Corresponding Author

Jitendra K. Bera – Department of Chemistry and Center for Environmental Science and Engineering, Indian Institute of Technology Kanpur, Kanpur 208016, India; orcid.org/0000-0002-5689-8863; Email: jbera@iitk.ac.in

Authors

Suman Yadav – Department of Chemistry and Center for Environmental Science and Engineering, Indian Institute of Technology Kanpur, Kanpur 208016, India

Indranil Dutta – Department of Chemistry and Center for Environmental Science and Engineering, Indian Institute of Technology Kanpur, Kanpur 208016, India

Sayantani Saha – Department of Chemistry and Center for Environmental Science and Engineering, Indian Institute of Technology Kanpur, Kanpur 208016, India

Shubhajit Das – New Chemistry Unit, School of Advanced Materials (SAMat), Jawaharlal Nehru Center for Advanced Scientific Research, Bangalore 560064, India

Swapan K. Pati – New Chemistry Unit, School of Advanced Materials (SAMat), Jawaharlal Nehru Center for Advanced Scientific Research, Bangalore 560064, India; orcid.org/0000-0002-5124-7455

Joyanta Choudhury – Organometallics & Smart Materials Laboratory, Department of Chemistry, Indian Institute of Science Education and Research Bhopal, Bhopal 462066, India; orcid.org/0000-0003-4776-8757

Complete contact information is available at:

<https://pubs.acs.org/doi/10.1021/acs.organomet.0c00413>

Notes

The authors declare no competing financial interest.

■ ACKNOWLEDGMENTS

Financial support from the Science and Engineering Research Board (SERB), the Department of Atomic Energy (DAE), and

the Indo-French Centre for the Promotion of Advanced Research (IFCPAR) is gratefully appreciated. J.K.B. and S.K.P. thank the SERB, DST, for J. C. Bose Fellowships. S.Y. thanks the UGC, India, for a fellowship. S.D. thanks the CSIR, India, and the JNCASR for fellowships. This paper is dedicated to P. H. Dixneuf for his outstanding contributions to organometallic chemistry.

■ REFERENCES

- (1) For recent reviews on metal NHC compounds, see: (a) Peris, E. Smart N-Heterocyclic Carbene Ligands in Catalysis. *Chem. Rev.* **2018**, *118*, 9988–10031. (b) Vivancos, A.; Segarra, C.; Albrecht, M. Mesoionic and Related Less Heteroatom Stabilized N-Heterocyclic Carbene Complexes: Synthesis, Catalysis, and Other Applications. *Chem. Rev.* **2018**, *118*, 9493–9586. (c) Huynh, H. V. Electronic Properties of N-Heterocyclic Carbenes and Their Experimental Determination. *Chem. Rev.* **2018**, *118*, 9457–9492. (d) Merics, L.; Albrecht, M. Beyond catalysis: N-heterocyclic Carbene Complexes as Components for Medicinal, Luminescent, and Functional Materials Applications. *Chem. Soc. Rev.* **2010**, *39*, 1903–1912. (e) Hopkinson, M. N.; Richter, C.; Schedler, M.; Glorius, F. An Overview of N-heterocyclic Carbenes. *Nature* **2014**, *510*, 485–496. (f) Huynh, H. V. *The Organometallic Chemistry of N-heterocyclic Carbenes*; Wiley: Chichester, United Kingdom, 2017. . Selected references for chemical transformation reactions with metal NHC complexes: (g) Diez-González, S.; Marion, N.; Nolan, S. P. N-Heterocyclic Carbenes in Late Transition Metal Catalysis. *Chem. Rev.* **2009**, *109*, 3612–3676. (h) Grubbs, R. H. Olefin Metathesis Catalysts for the Preparation of Molecules and Materials (Nobel Lecture). *Angew. Chem., Int. Ed.* **2006**, *45*, 3760–3765. (i) Crabtree, R. H. NHC Ligands versus Cyclopentadienyls and Phosphines as Spectator Ligands in Organometallic Catalysis. *J. Organomet. Chem.* **2005**, *690*, S451–S457. (j) Herrmann, W. A. N-Heterocyclic Carbenes: A New Concept in Organometallic Catalysis. *Angew. Chem., Int. Ed.* **2002**, *41*, 1290–1309. (k) Trnka, T. M.; Grubbs, R. H. The Development of L₂X₂Ru=CHR Olefin Metathesis Catalysts: An Organometallic Success Story. *Acc. Chem. Res.* **2001**, *34*, 18–29. (l) Jin, H.; Mück-Lichtenfeld, C.; Hepp, A.; Stephan, D. W.; Hahn, F. E. Small Molecule Activation with N,NR-MIC Platinum Complexes. *Chem. - Eur. J.* **2017**, *23*, S943–S947. (m) Mata, J. A.; Hahn, F. E.; Peris, E. Heterometallic Complexes, Tandem Catalysis and Catalytic Cooperativity. *Chem. Sci.* **2014**, *5*, 1723–1732.
- (2) For selected examples of mesoionic carbene complexes, see: (a) Kluser, E.; Neels, A.; Albrecht, M. Mild and Rational Synthesis of Palladium Complexes Comprising C(4)-bound N-heterocyclic Carbenes. *Chem. Commun.* **2006**, 4495–4497. (b) Albrecht, M. C4-bound Imidazolylidenes: from Curiosities to High Impact Carbene Ligands. *Chem. Commun.* **2008**, 3601–3610. (c) Albrecht, M.; Cavell, K. J. Abnormal NHCs: Coordination, Reaction Chemistry and Catalytic Applications. *Organomet. Chem.* **2009**, *35*, 47–61. For reviews on mesoionic carbenes, see: (d) Arnold, P. L.; Pearson, S. Abnormal N-heterocyclic Carbenes. *Coord. Chem. Rev.* **2007**, *251*, 596–609. (e) Crabtree, R. H. Abnormal, Mesoionic and Remote N-heterocyclic Carbene Complexes. *Coord. Chem. Rev.* **2013**, *257*, 755–766. (f) Schuster, O.; Yang, L.; Raubenheimer, H. G.; Albrecht, M. Beyond Conventional N-Heterocyclic Carbenes: Abnormal, Remote, and Other Classes of NHC Ligands with Reduced Heteroatom Stabilization. *Chem. Rev.* **2009**, *109*, 3445–3478.
- (3) For NHC metal complex catalyzed oxidation reactions, see: (a) Konnick, M. M.; Guzei, I. A.; Stahl, S. S. Characterization of Peroxo and Hydroperoxo Intermediates in the Aerobic Oxidation of N-Heterocyclic Carbene Coordinated Palladium(0). *J. Am. Chem. Soc.* **2004**, *126*, 10212–10213. (b) Poyatos, M.; Mata, J. A.; Falomir, E.; Crabtree, R. H.; Peris, E. New Ruthenium(II) CNC-Pincer Bis(carbene) Complexes: Synthesis and Catalytic Activity. *Organometallics* **2003**, *22*, 1110–1114. (c) Schultz, M. J.; Hamilton, S. S.; Jensen, D. R.; Sigman, M. S. Development and Comparison of the Substrate Scope of Pd-Catalysts for the Aerobic Oxidation of

Alcohols. *J. Org. Chem.* **2005**, *70*, 3343–3352. (d) Daw, P.; Petakamsetty, R.; Sarbajna, A.; Laha, S.; Ramapanicker, R.; Bera, J. K. A Highly Efficient Catalyst for Selective Oxidative Scission of Olefins to Aldehydes: Abnormal NHC–Ru(II) Complex in Oxidation Chemistry. *J. Am. Chem. Soc.* **2014**, *136*, 13987–13990.

(4) Selected examples: (a) Knowles, W. S. Asymmetric Hydrogenations (Nobel Lecture). *Angew. Chem., Int. Ed.* **2002**, *41*, 1998–2007. (b) Noyori, R. Asymmetric Catalysis: Science and Opportunities (Nobel Lecture). *Angew. Chem., Int. Ed.* **2002**, *41*, 2008–2022. (c) Powell, M. T.; Hou, D.-R.; Perry, M. C.; Cui, X.; Burgess, K. Chiral Imidazolylidene Ligands for Asymmetric Hydrogenation of Aryl Alkenes. *J. Am. Chem. Soc.* **2001**, *123*, 8878–8879. (d) Sprengers, J. W.; Wassenaar, J.; Clement, N. D.; Cavell, K. J.; Elsevier, C. J. Palladium–(N-Heterocyclic Carbene) Hydrogenation Catalysts. *Angew. Chem., Int. Ed.* **2005**, *44*, 2026–2029. (e) Baskakov, D.; Herrmann, W. A.; Herdtweck, E.; Hoffmann, S. D. Chiral N-Heterocyclic Carbenes with Restricted Flexibility in Asymmetric Catalysis. *Organometallics* **2007**, *26*, 626–632. (f) Chen, D.; Banphavichit, V.; Reibenspies, J.; Burgess, K. New Optically Active N-Heterocyclic Carbene Complexes for Hydrogenation: A Tale with an Atropisomeric Twist. *Organometallics* **2007**, *26*, 855–859. (g) Camm, K. D.; Castro, N. M.; Liu, Y.; Czechura, P.; Snelgrove, J. L.; Fogg, D. E. Tandem ROMP Hydrogenation with a Third Generation Grubbs Catalyst. *J. Am. Chem. Soc.* **2007**, *129*, 4168–4169. (h) Siek, S.; Burks, D. B.; Gerlach, D. L.; Liang, G.; Tesh, J. M.; Thompson, C. R.; Qu, F.; Shankwitz, J. E.; Vasquez, R. M.; Chambers, N.; Szulczewski, G. J.; Grotjahn, D. B.; Webster, C. E.; Papish, E. T. Iridium and Ruthenium Complexes of N-Heterocyclic Carbene- and Pyridinol-Derived Chelates as Catalysts for Aqueous Carbon Dioxide Hydrogenation and Formic Acid Dehydrogenation: The Role of the Alkali Metal. *Organometallics* **2017**, *36*, 1091–1106.

(5) (a) Gandolfi, C.; Heckenroth, M.; Neels, A.; Laurenczy, G.; Albrecht, M. Chelating NHC Ruthenium(II) Complexes as Robust Homogeneous Hydrogenation Catalysts. *Organometallics* **2009**, *28*, 5112–5121. (b) Jazsar, R. F. R.; Macgregor, S. A.; Mahon, M. F.; Richards, S. P.; Whittlesey, M. K. C–C and C–H Bond Activation Reactions in N-Heterocyclic Carbene Complexes of Ruthenium. *J. Am. Chem. Soc.* **2002**, *124*, 4944–4945. (c) McGuinness, D. S.; Saendig, N.; Yates, B. F.; Cavell, K. J. Kinetic and Density Functional Studies on Alkyl Carbene Elimination from Pd^{II} Heterocyclic Carbene Complexes: A New Type of Reductive Elimination with Clear Implications for Catalysis. *J. Am. Chem. Soc.* **2001**, *123*, 4029–4040. (d) Saker, O.; Mahon, M. F.; Warren, J. E.; Whittlesey, M. K. Sequential Formation of [Ru(IPr)₂(CO)H(OH₂)]⁺ and [Ru(IPr)(η^5 -C₆H₆)(CO)H]⁺ upon Protonation of Ru(IPr)₂(CO)H(OH) (IPr = 1,3-bis(2,6-diisopropylphenyl)imidazol-2-ylidene). *Organometallics* **2009**, *28*, 1976–1979. (e) Normand, A. T.; Yen, S. K.; Huynh, H. V.; Hor, T. S. A.; Cavell, K. J. Catalytic Annulation of Heterocycles via a Novel Redox Process Involving the Imidazolium Salt N-Heterocyclic Carbene Couple. *Organometallics* **2008**, *27*, 3153–3160. (f) Chantler, V. L.; Chatwin, S. L.; Jazsar, R. F. R.; Mahon, M. F.; Saker, O.; Whittlesey, M. K. Stoichiometric and Catalytic Reactivity of the N-heterocyclic Ruthenium Hydride Complexes [Ru(NHC)(L)(CO)HCl] and [Ru(NHC)(L)(CO)H(η^2 -BH₄)] (L = NHC, PPh₃). *Dalton Trans.* **2008**, 2603–2614.

(6) For reviews on chelation in NHC ligands, see: (a) Peris, E.; Crabtree, R. H. Recent Homogeneous Catalytic Applications of Chelate and Pincer N-heterocyclic Carbenes. *Coord. Chem. Rev.* **2004**, *248*, 2239–2246. (b) Köhl, O. The Chemistry of Functionalised N-heterocyclic Carbenes. *Chem. Soc. Rev.* **2007**, *36*, 592–607. (c) Liddle, S. T.; Edworthy, I. S.; Arnold, P. L. Anionic Tethered N-heterocyclic Carbene Chemistry. *Chem. Soc. Rev.* **2007**, *36*, 1732–1744. (d) Hameury, S.; de Fremont, P.; Braunstein, P. Metal complexes with oxygen-functionalized NHC ligands: synthesis and applications. *Chem. Soc. Rev.* **2017**, *46*, 632–733.

(7) Lead references for annelated NHCs: (a) Reshi, N. D.; Bera, J. K. Recent Advances in Anellated NHCs and their Metal Complexes. *Coord. Chem. Rev.* **2020**, *422*, 213334. (b) Gierz, V.; Maichle-Mössmer, C.; Kunz, D. 1,10-Phenanthroline Analogue Pyridazine

Based N-Heterocyclic Carbene Ligands. *Organometallics* **2012**, *31*, 739–747. (c) Alcarazo, M.; Roseblade, S. J.; Cowley, A. R.; Fernández, R.; Brown, J. M.; Lassaletta, J. M. Imidazo[1,5-*a*]pyridine: A Versatile Architecture for Stable N-Heterocyclic Carbenes. *J. Am. Chem. Soc.* **2005**, *127*, 3290–3291. (d) Song, G.; Zhang, Y.; Li, X. Rhodium and Iridium Complexes of Abnormal N-Heterocyclic Carbenes Derived from Imidazo[1,2-*a*]pyridine. *Organometallics* **2008**, *27*, 1936–1943. (e) Saravanakumar, S.; Oprea, A. I.; Kindermann, M. K.; Jones, P. G.; Heinicke, J. Anellated N-Heterocyclic Carbenes: 1,3-Dineopentylphtho[2,3-*d*]imidazol-2-ylidene: Synthesis, KOH Addition Product, Transition Metal Complexes, and Anellation Effects. *Chem. - Eur. J.* **2006**, *12*, 3143–3154.

(8) Selected examples: (a) Kriechbaum, M.; List, M.; Berger, R. J. F.; Patzschke, M.; Monkowius, U. Silver and Gold Complexes with a New 1,10-Phenanthroline Analogue N-Heterocyclic Carbene: A Combined Structural, Theoretical, and Photophysical Study. *Chem. - Eur. J.* **2012**, *18*, 5506–5509. (b) Phukan, A. K.; Guha, A. K.; Sarmah, S.; Dewhurst, R. D. Electronic and Ligand Properties of Anellated Normal and Abnormal (Mesoionic) N Heterocyclic Carbenes: A Theoretical Study. *J. Org. Chem.* **2013**, *78*, 11032–11039. (c) Sanderson, M. D.; Kamplain, J. W.; Bielawski, C. W. Quinone-Annulated N-Heterocyclic Carbene-Transition-Metal Complexes: Observation of π -Backbonding Using FT-IR Spectroscopy and Cyclic Voltammetry. *J. Am. Chem. Soc.* **2006**, *128*, 16514–16515. (d) Suresh, C. H.; Ajitha, M. J. DFT Prediction of Multitopic N Heterocyclic Carbenes Using Clar's Aromatic Sextet Theory. *J. Org. Chem.* **2013**, *78*, 3918–3924.

(9) Saha, S.; Daw, P.; Bera, J. K. Oxidative Route to Abnormal NHC Compounds from Singly-Bonded [M–M] (M = Ru, Rh, Pd) Precursors. *Organometallics* **2015**, *34*, 5509–5512.

(10) For semihydrogenation of alkynes, see the following references and literature cited therein: (a) De Vries, J. G.; Elsevier, C. J. *Handbook of Homogeneous Hydrogenation*; Wiley-VCH: Weinheim, Germany, 2007. (b) Blaser, H.-U.; Schnyder, A.; Steiner, H.; Rössler, F.; Baumeister, P. In *Handbook of Heterogeneous Catalysis*, 2nd ed.; Ertl, G.; Knözinger, H.; Schüth, F.; Weitkamp, J., Eds.; Wiley-VCH: Weinheim, Germany, 2008; Vol. 7, pp 3284–3308. (c) Rylander, P. N. *Catalytic Hydrogenation in Organic Syntheses*; Academic Press: New York, 1979. (d) Chaloner, P. A.; Esteruelas, M. A.; Joo, F.; Oro, L. A. In *Homogeneous Hydrogenation*; Ugo, R., James, B. R., Eds.; Kluwer Academic: Dordrecht, The Netherlands, 1993. (e) Oger, C.; Balas, L.; Durand, T.; Galano, J.-M. Are Alkyne Reductions Chemo-, Regio-, and Stereoselective Enough to Provide Pure Z-Olefins in Polyfunctionalized Bioactive Molecules. *Chem. Rev.* **2013**, *113*, 1313–1350. (f) Chinchilla, R.; Najera, C. Chemicals from Alkynes with Palladium Catalysts. *Chem. Rev.* **2014**, *114*, 1783–1826. (g) Furukawa, S.; Komatsu, T. Selective Hydrogenation of Functionalized Alkynes to (E)-Alkenes, Using Ordered Alloys as Catalysts. *ACS Catal.* **2016**, *6*, 2121–2125. (h) Desai, S. P.; Ye, J.; Zheng, J.; Ferrandon, M. S.; Webber, T. E.; Platero-Prats, A. E.; Duan, J.; Garcia-Holley, P.; Camaioni, D. M.; Chapman, K. W.; Delferro, M.; Farha, O. K.; Fulton, J. L.; Gagliardi, L.; Lercher, J. A.; Penn, R. L.; Stein, A.; Lu, C. C. Well Defined Rhodium–Gallium Catalytic Sites in a Metal–Organic Framework: Promoter-Controlled Selectivity in Alkyne Semihydrogenation to E- Alkenes. *J. Am. Chem. Soc.* **2018**, *140*, 15309–15318. (i) Ramirez, B. L.; Lu, C. C. Rare-Earth Supported Nickel Catalysts for Alkyne Semihydrogenation: Chemo- and Regioselectivity Impacted by the Lewis Acidity and Size of the Support. *J. Am. Chem. Soc.* **2020**, *142*, 5396–5407. (j) Swamy, K. C. K.; Reddy, A. S.; Sandeep, K.; Kalyani, A. Advances in chemoselective and/or stereoselective semihydrogenation of alkynes. *Tetrahedron Lett.* **2018**, *59*, 419–429.

(11) For Z-selective homogeneous semihydrogenation methods, see: (a) Van Laren, M. W.; Elsevier, C. J. Selective Homogeneous Palladium(0) Catalyzed Hydrogenation of Alkynes to Z-Alkenes. *Angew. Chem., Int. Ed.* **1999**, *38*, 3715–3717. (b) Hauwert, P.; Maestri, G.; Sprengers, J. W.; Catellani, M.; Elsevier, C. J. Transfer Semihydrogenation of Alkynes Catalyzed by a Zero Valent Palladium

- N-Heterocyclic Carbene Complex. *Angew. Chem., Int. Ed.* **2008**, *47*, 3223–3226. (c) La Pierre, H. S.; Arnold, J.; Toste, F. D. Z-Selective Semihydrogenation of Alkynes Catalyzed by a Cationic Vanadium Bisimido Complex. *Angew. Chem., Int. Ed.* **2011**, *50*, 3900–3903. (d) Warsink, S.; Bosman, S.; Weigand, J. J.; Elsevier, C. J. Rigid Pyridyl Substituted NHC Ligands, their Pd(0) Complexes and their Application in Selective Transfer Semihydrogenation of Alkynes. *Appl. Organomet. Chem.* **2011**, *25*, 276–282. (e) Drost, R. M.; Bouwens, T.; van Leest, N. P.; de Bruin, B.; Elsevier, C. J. Convenient Transfer Semihydrogenation Methodology for Alkynes Using a Pd(II)-NHC Precatalyst. *ACS Catal.* **2014**, *4*, 1349–1357. (f) Drost, R. M.; Broere, D. L. J.; Hoogenboom, J.; de Baan, S. N.; Lutz, M.; de Bruin, B.; Elsevier, C. J. Allyl-palladium(II) Histidylidene Complexes and Their Application in Z-Selective Transfer Semihydrogenation of Alkynes. *Eur. J. Inorg. Chem.* **2015**, *2015*, 982–996. (g) Chen, C.; Huang, Y.; Zhang, Z.; Dong, X.-Q.; Zhang, X. Cobalt-Catalyzed Z-Selective Semihydrogenation of Alkynes with Molecular Hydrogen. *Chem. Commun.* **2017**, *53*, 4612–4615. (h) Korytia-ková, E.; Thiel, N. O.; Pape, F.; Teichert, J. F. Copper(I)-Catalyzed Transfer Hydrogenations with Ammonia Borane. *Chem. Commun.* **2017**, *53*, 732–735. (i) Brzozowska, A.; Azofra, L. M.; Zubar, V.; Atodiresei, I.; Cavallo, L.; Rueping, M.; El-Sepelgy, O. Highly Chemo- and Stereoselective Transfer Semihydrogenation of Alkynes Catalyzed by a Stable, Well Defined Manganese(II) Complex. *ACS Catal.* **2018**, *8*, 4103–4109. (j) Johnson, C.; Albrecht, M. Z-Selective Alkyne Semihydrogenation Catalyzed by Piano Stool N-heterocyclic Carbene Iron Complexes. *Catal. Sci. Technol.* **2018**, *8*, 2779–2783. (k) Osborn, J. A.; Jardine, F. H.; Young, J. F.; Wilkinson, G. The Preparation and Properties of Tris(Triphenylphosphine)-Halogenorhodium(I) and Some Reactions Thereof Including Catalytic Homogeneous Hydrogenation of Olefins and Acetylenes and Their Derivatives. *J. Chem. Soc. A* **1966**, 1711–1732. (l) Tseng, K.-N. T.; Kampf, J. W.; Szymczak, N. K. Modular Attachment of Appended Boron Lewis Acids to a Ruthenium Pincer Catalyst: Metal–Ligand Cooperativity Enables Selective Alkyne Hydrogenation. *J. Am. Chem. Soc.* **2016**, *138*, 10378–10381.
- (12) For Z-selective heterogeneous semihydrogenation methods, see: (a) Mitsudome, T.; Takahashi, Y.; Ichikawa, S.; Mizugaki, T.; Jitsukawa, K.; Kaneda, K. Metal–Ligand Core–Shell Nanocomposite Catalysts for the Selective Semihydrogenation of Alkynes. *Angew. Chem., Int. Ed.* **2013**, *52*, 1481–1485. (b) Gieshoff, T. N.; Welther, A.; Kessler, M. T.; Precht, M. H. G.; Wangelin, A. J. V. Stereoselective Iron Catalyzed Alkyne Hydrogenation in Ionic Liquids. *Chem. Commun.* **2014**, *50*, 2261–2264. (c) Vasilikogiannaki, E.; Titilas, I.; Vassilikogiannakis, G.; Stratakis, M. Cis-Semihydrogenation of Alkynes with Amine Borane Complexes Catalyzed by Gold Nano particles under Mild Conditions. *Chem. Commun.* **2015**, *51*, 2384–2387. (d) Mitsudome, T.; Yamamoto, M.; Maeno, Z.; Mizugaki, T.; Jitsukawa, K.; Kaneda, K. One step Synthesis of Core-Gold/Shell-Ceria Nanomaterial and Its Catalysis for Highly Selective Semihydrogenation of Alkynes. *J. Am. Chem. Soc.* **2015**, *137*, 13452–13455. (e) Mitsudome, T.; Urayama, T.; Yamazaki, K.; Maehara, Y.; Yamasaki, J.; Gohara, K.; Maeno, Z.; Mizugaki, T.; Jitsukawa, K.; Kaneda, K. Design of Core-Pd/Shell-Ag Nanocomposite Catalyst for Selective Semihydrogenation of Alkynes. *ACS Catal.* **2016**, *6*, 666–670. (f) Konnerth, H.; Precht, M. H. G. Selective Partial Hydrogenation of Alkynes To Z-Alkenes with Ionic Liquid-Doped Nickel Nanocatalysts at Near Ambient Conditions. *Chem. Commun.* **2016**, *52*, 9129–9132. (g) Delgado, J. A.; Ben kirane, O.; Claver, C.; Curulla-Ferré, D.; Godard, C. Advances in the Preparation of Highly Selective Nanocatalysts for the Semihydrogenation of Alkynes Using Colloidal Approaches. *Dalton Trans.* **2017**, *46*, 12381–12403. (h) Chen, F.; Kreyenschulte, C.; Radnik, J.; Lund, H.; Surkus, A.-E.; Junge, K.; Beller, M. Selective Semihydrogenation of Alkynes with N Graphitic-Modified Cobalt Nanoparticles Supported on Silica. *ACS Catal.* **2017**, *7*, 1526–1532. (i) Fiorio, J. L.; López, N.; Rossi, L. M. Gold–Ligand Catalyzed Selective Hydrogenation of Alkynes into *cis*-Alkenes via H₂ Heterolytic Activation by Frustrated Lewis Pairs. *ACS Catal.* **2017**, *7*, 2973–2980. (j) Lu, Y.; Feng, X.; Takale, B. S.; Yamamoto, Y.; Zhang, W.; Bao, M. Highly Selective Semihydrogenation of Alkynes to Alkenes by Using an Unsupported Nanoporous Palladium Catalyst: No Leaching of Palladium into the Reaction Mixture. *ACS Catal.* **2017**, *7*, 8296–8303. (k) Rej, S.; Madasu, M.; Tan, C.-S.; Hsia, C.-F.; Huang, M. H. Polyhedral Cu₂O to Cu Pseudomorphic Conversion for Stereoselective Alkyne Semihydrogenation. *Chem. Sci.* **2018**, *9*, 2517–2524. (l) Lindlar, H.; Dubuis, R. Palladium Catalyst for Partial Reduction of Acetylenes. *Org. Synth.* **2003**, *46*, 89.
- (13) Pasto, D. J. In *Comprehensive Organic Synthesis*; Trost, B. M., Fleming, I., Eds.; Pergamon: Oxford, U.K., 1991; Vol. 8, p 471.
- (14) For selective synthesis of (E)-alkenes via transfer hydrogenation, see: (a) Alshakova, I. D.; Gabidullin, B.; Nikonov, G. I. Ru-Catalyzed Transfer Hydrogenation of Nitriles, Aromatics, Olefins, Alkynes and Esters. *ChemCatChem* **2018**, *10*, 4860–4869. (b) Wang, Y.; Huang, Z.; Leng, X.; Zhu, H.; Liu, G.; Huang, Z. Transfer Hydrogenation of Alkenes Using Ethanol Catalyzed by a NCP Pincer Iridium Complex: Scope and Mechanism. *J. Am. Chem. Soc.* **2018**, *140*, 4417–4429. (c) Reddy, A. S.; Swamy, K. C. K. Ethanol as a Hydrogenating Agent: Palladium-Catalyzed Stereoselective Hydrogenation of Ynamides To Give Enamides. *Angew. Chem., Int. Ed.* **2017**, *56*, 6984–6988. (d) Cummings, S. P.; Le, T.-N.; Fernandez, G. E.; Quimbao, L. G.; Stokes, B. J. Tetrahydroxydiboron-Mediated Palladium-Catalyzed Transfer Hydrogenation and Deuteration of Alkenes and Alkynes Using Water as the Stoichiometric H or D Atom Donor. *J. Am. Chem. Soc.* **2016**, *138*, 6107–6110. (e) Luo, F.; Pan, C.; Wang, W.; Ye, Z.; Cheng, J. Palladium Catalyzed Reduction of Alkynes Employing HSiEt₃: Stereoselective Synthesis of *trans*- and *cis*-Alkenes. *Tetrahedron* **2010**, *66*, 1399–1403. (f) Shirakawa, E.; Otsuka, H.; Hayashi, T. Reduction of Alkynes into 1,2-dideuterioalkenes with Hexamethyldisilane and Deuterium Oxide in the Presence of a Palladium Catalyst. *Chem. Commun.* **2005**, 5885–5886.
- (15) Tani, K.; Iseki, A.; Yamagata, T. Efficient Transfer Hydrogenation of Alkynes and Alkenes with Methanol Catalyzed by Hydrido(methoxy)-Iridium(III) Complexes. *Chem. Commun.* **1999**, 1821–1822.
- (16) (a) Trost, B. M.; Ball, Z. T.; Jöge, T. A Chemoselective Reduction of Alkynes to *E*-Alkenes. *J. Am. Chem. Soc.* **2002**, *124*, 7922–7923. (b) Trost, B. M.; Machacek, M. R.; Ball, Z. T. Ruthenium-Catalyzed Vinylsilane Synthesis and Cross-Coupling as a Selective Approach to Alkenes: Benzyltrimethylsilyl as a Robust Vinylmetal Functionality. *Org. Lett.* **2003**, *5*, 1895–1898. (c) Trost, B. M.; Ball, Z. T. Addition of Metalloid Hydrides to Alkynes: Hydrometallation with Boron, Silicon, and Tin. *Synthesis* **2005**, *2005*, 853–887.
- (17) (a) Chen, T.; Xiao, J.; Zhou, Y.; Yin, S.; Han, L.-B. Nickel-catalyzed *E*-selective semihydrogenation of internal alkynes with hypophosphorous acid. *J. Organomet. Chem.* **2014**, *749*, 51–54. (b) Richmond, E.; Moran, J. Ligand Control of *E/Z* Selectivity in Nickel-Catalyzed Transfer Hydrogenative Alkyne Semireduction. *J. Org. Chem.* **2015**, *80*, 6922–6929. (c) Shen, R.; Chen, T.; Zhao, Y.; Qiu, R.; Yin, S.; Wang, X.; Goto, M.; Han, L.-B. Facile Regio- and Stereo-selective Hydrometallation of Alkynes with a Combination of Carboxylic Acids and Group 10 Transition Metal Complexes: Selective Hydrogenation of Alkynes with Formic Acid. *J. Am. Chem. Soc.* **2011**, *133*, 17037–17044. (d) Li, J.; Hua, R. Stereodivergent Ruthenium-Catalyzed Transfer Semihydrogenation of Diaryl Alkynes. *Chem. - Eur. J.* **2011**, *17*, 8462–8465. (e) Musa, S.; Ghosh, A.; Vaccaro, L.; Ackermann, L.; Gelman, D. Efficient *E*-Selective Transfer Semihydrogenation of Alkynes by Means of Ligand-Metal Cooperating Ruthenium Catalyst. *Adv. Synth. Catal.* **2015**, *357*, 2351–2357. (f) Broggi, J.; Jurčík, V.; Songis, O.; Poater, A.; Cavallo, L.; Slawin, A. M. Z.; Cazin, C. S. J. The Isolation of [Pd{OC(O)H}(H)(NHC)-(PR₃)] (NHC = N-Heterocyclic Carbene) and Its Role in Alkene and Alkyne Reductions Using Formic Acid. *J. Am. Chem. Soc.* **2013**, *135*, 4588–4591.
- (18) Fu, S.; Chen, N.-Y.; Liu, X.; Shao, Z.; Luo, S.-P.; Liu, Q. Ligand Controlled Cobalt-Catalyzed Transfer Hydrogenation of Alkynes:

Stereodivergent Synthesis of *Z*- and *E*-Alkenes. *J. Am. Chem. Soc.* **2016**, *138*, 8588–8594.

(19) Yang, J.; Wang, C.; Sun, Y.; Man, X.; Li, J.; Sun, F. Ligand-controlled iridium-catalyzed semihydrogenation of alkynes with ethanol: highly stereoselective synthesis of *E*- and *Z*-alkenes. *Chem. Commun.* **2019**, *55*, 1903–1906.

(20) Ekebergh, A.; Begon, R.; Kann, N. Ruthenium-Catalyzed *E*-Selective Alkyne Semihydrogenation with Alcohols as Hydrogen Donors. *J. Org. Chem.* **2020**, *85*, 2966–2975.

(21) Schleyer, D.; Niessen, H. G.; Bargon, J. In situ ^1H -PHIP NMR Studies of the Stereoselective Hydrogenation of Alkynes to *E*-alkenes Catalyzed by a Homogeneous $[\text{Cp}^*\text{Ru}]^+$ Catalyst. *New J. Chem.* **2001**, *25*, 423–426.

(22) Radkowski, K.; Sundararaju, B.; Fürstner, A. A Functional Group Tolerant Catalytic *trans* Hydrogenation of Alkynes. *Angew. Chem., Int. Ed.* **2013**, *52*, 355–360.

(23) Srimani, D.; Diskin-Posner, Y.; Ben-David, Y.; Milstein, D. Iron Pincer Complex Catalyzed, Environmentally Benign, *E*-selective Semihydrogenation of Alkynes. *Angew. Chem., Int. Ed.* **2013**, *52*, 14131–14134.

(24) Tokmic, K.; Fout, A. R. Alkyne Semihydrogenation with a Well Defined Nonclassical $\text{Co}-\text{H}_2$ Catalyst: A H_2 Spin on Isomerization and *E*-Selectivity. *J. Am. Chem. Soc.* **2016**, *138*, 13700–13705.

(25) Murugesan, K.; Bheeter, C. B.; Linnebank, P. R.; Spannenberg, A.; Reek, J. N. H.; Jagadeesh, R. V.; Beller, M. Nickel-Catalyzed Stereodivergent Synthesis of *E*- and *Z*-Alkenes by Hydrogenation of Alkynes. *ChemSusChem* **2019**, *12*, 3363–3369.

(26) Bimetallic catalysts for homogeneous alkyne semihydrogenation: (a) Karunananda, M. K.; Mankad, N. P. *E*-Selective Semihydrogenation of Alkynes by Heterobimetallic Catalysis. *J. Am. Chem. Soc.* **2015**, *137*, 14598–14601. (b) Higashida, K.; Mashima, K. *E*-Selective Semi-hydrogenation of Alkynes with Dinuclear Iridium Complexes under Atmospheric Pressure of Hydrogen. *Chem. Lett.* **2016**, *45*, 866–868. (c) Takemoto, S.; Kitamura, M.; Saruwatari, S.; Isono, A.; Takada, Y.; Nishimori, R.; Tsujiwaki, M.; Sakaue, N.; Matsuzaka, H. Bis(bipyridine) ruthenium(II) bis(phosphido)-metalloligand: synthesis of heterometallic complexes and application to catalytic *E*-selective alkyne semihydrogenation. *Dalton Trans.* **2019**, *48*, 1161–1165.

(27) For metal vinylidene complexes, see: (a) Silvestre, J.; Hoffmann, R. Hydrogen Migration in Transition Metal Alkyne and Related Complexes. *Helv. Chim. Acta* **1985**, *68*, 1461–1506. (b) Dragutan, V.; Dragutan, I. Ruthenium Vinylidene Complexes. *Platinum Met. Rev.* **2004**, *48*, 148–153. (c) Cowley, M. J.; Lynam, J. M.; Slattery, J. M. A Mechanistic Study in to the Interconversion of Rhodium Alkyne, Alkynyl Hydride and Vinylidene Complexes. *Dalton Trans.* **2008**, 4552–4554. (d) Bruneau, C.; Dixneuf, P. H. Metal Vinylidenes in Catalysis. *Acc. Chem. Res.* **1999**, *32*, 311–323. (e) Grotjahn, D. B.; Zeng, Xi.; Cooksy, A. L. Alkyne-to-Vinylidene Transformation on *trans*-(Cl)Rh(phosphine) $_2$: Acceleration by a Heterocyclic Ligand and Absence of Bimolecular Mechanism. *J. Am. Chem. Soc.* **2006**, *128*, 2798–2799. (f) Grotjahn, D. B.; Zeng, Xi.; Cooksy, A. L.; Kassel, W. S.; DiPasquale, A. G.; Zakharov, L. N.; Rheingold, A. L. Experimental and Computational Study of the Transformation of Terminal Alkynes to Vinylidene Ligands on *trans*-(Chloro)bis(phosphine)Rh Fragments and Effects of Phosphine Substituents. *Organometallics* **2007**, *26*, 3385–3402.

(28) Selected examples: (a) Saha, S.; Sarbajna, A.; Bera, J. K. Bulky, Spherical, and Fluorinated Anion BAR^{F} Induces ‘on-water’ Activity of Silver Salt for The Hydration of Terminal Alkynes. *Tetrahedron Lett.* **2014**, *55*, 1444–1447. (b) Marion, N.; Ramón, R. S.; Nolan, S. P. $[(\text{NHC})\text{AuI}]$ Catalyzed Acid Free Alkyne Hydration at Part-per-Million Catalyst Loadings. *J. Am. Chem. Soc.* **2009**, *131*, 448–449. (c) Meier, I. K.; Marsella, J. A. Hydration of Acetylenic Compounds Without Using Mercury. *J. Mol. Catal.* **1993**, *78*, 31–42. (d) Thuong, M. B. T.; Mann, A.; Wagner, A. Mild Chemoselective Hydration of Terminal Alkynes Catalyzed by AgSbF_6 . *Chem. Commun.* **2012**, *48*, 434–436. (e) Das, R.; Chakraborty, D. AgOTf Catalyzed Hydration of Terminal Alkynes. *Appl. Organomet. Chem.* **2012**, *26*, 722–726.

(f) Rao, K. T. V.; Prasad, P. S. S.; Lingaiah, N. Solvent free Hydration of Alkynes Over a Heterogeneous Silver Exchanged Silico Tungstic Acid Catalyst. *Green Chem.* **2012**, *14*, 1507–1514.

(29) (a) Giboulot, S.; Baldino, S.; Ballico, M.; Nedden, H. G.; Zuccaccia, D.; Baratta, W. Cyclometalated Dicarboxyl Ruthenium Catalysts for Transfer Hydrogenation and Hydrogenation of Carbonyl Compounds. *Organometallics* **2018**, *37*, 2136–2146. (b) Giboulot, S.; Baldino, S.; Ballico, M.; Figliolia, R.; Pöthig, A.; Zhang, S.; Zuccaccia, D.; Baratta, W. Flat and Efficient HCN and CNN Pincer Ruthenium Catalysts for Carbonyl Compound Reduction. *Organometallics* **2019**, *38*, 1127–1142.

(30) (a) Hill, D. E.; Pei, Q.-L.; Zhang, E.-X.; Gage, J. R.; Yu, J.-Q.; Blackmond, D. G. A General Protocol for Addressing Speciation of the Active Catalyst Applied to Ligand-Accelerated Enantioselective $\text{C}(\text{sp}^3)$ – H Bond Arylation. *ACS Catal.* **2018**, *8*, 1528–1531. (b) Moene, W.; Vos, M.; Schakel, M.; de Kanter, F. J. J.; Schmitz, R. F.; Klumpp, G. W. Reactivity of Ether- and Amine-Complexed Dimers and Tetramers of Alkylolithiums towards Triphenylmethane. *Chem. - Eur. J.* **2000**, *6*, 225–236. (c) Luitjes, H.; de Kanter, F. J. J.; Schakel, M.; Schmitz, R. F.; Klumpp, G. W. Lewis Base Complexation, Aggregation, and Reactivity of σ -Organolithiums. Significance of Fractional Reaction Orders in RL. *J. Am. Chem. Soc.* **1995**, *117*, 4179–4180.

(31) (a) Burch, R. R.; Muetterties, E. L.; Teller, R. G.; Williams, J. M. Selective Formation of *trans* Olefins by a Catalytic Hydrogenation of Alkynes Mediated at Two Adjacent Metal Centers. *J. Am. Chem. Soc.* **1982**, *104*, 4257–4258. (b) Burch, R. R.; Shusterman, A. J.; Muetterties, E. L.; Teller, R. G.; Williams, J. M. Coordinately Unsaturated Clusters. A Novel Catalytic Reaction. *J. Am. Chem. Soc.* **1983**, *105*, 3546–3556. (c) Suzuki, H.; Omori, H.; Lee, D. H.; Yoshida, Y.; Fukushima, M.; Tanaka, M.; Moro-oka, Y. Synthesis, Structure, and Chemistry of a Dinuclear Tetrahydride-Bridged Complex of Ruthenium, $(\eta^5\text{-C}_5\text{Me}_5)_2\text{Ru}(\mu\text{-H})_4\text{Ru}(\eta^5\text{-C}_5\text{Me}_5)$. C-H Bond Activation and Coupling Reaction of Ethylene on Dinuclear Complexes. *Organometallics* **1994**, *13*, 1129–1146. (d) Omori, H.; Suzuki, H.; Kakigano, T.; Moro-oka, Y. Synthesis and Molecular Structure of a Dinuclear Ruthenium Dihydride Complex Containing a Perpendicularly Bridging Diphenylacetylene Ligand. *Organometallics* **1992**, *11*, 989–992.

(32) (a) Hauwert, P.; Boerleider, R.; Warsink, S.; Weigand, J. J.; Elsevier, C. J. Mechanism of $\text{Pd}(\text{NHC})$ -Catalyzed Transfer Hydrogenation of Alkynes. *J. Am. Chem. Soc.* **2010**, *132*, 16900–16910. (b) Kluwer, A. M.; Koblenz, T. S.; Jonischkeit, T.; Woelk, K.; Elsevier, C. J. Kinetic and Spectroscopic Studies of the $[\text{Palladium}(\text{Ar-Bian})]$ Catalyzed Semihydrogenation of 4-Octyne. *J. Am. Chem. Soc.* **2005**, *127*, 15470–15480.

(33) Ogwen, A. O.; Ojwach, S. O.; Akerman, M. P. Cationic Pyridyl(benzoxazole) Ruthenium(II) Complexes: Efficient and Recyclable Catalysts in Biphasic Hydrogenation of Alkenes and Alkynes. *Appl. Catal., A* **2014**, *486*, 250–258.

(34) Zhao, Y.; Truhlar, D. G. The M06 Suite of Density Functionals for Main Group Thermochemistry, Thermochemical Kinetics, Noncovalent Interactions, Excited States, and Transition Elements: Two New Functionals and Systematic Testing of Four M06-class Functionals and 12 other Functionals. *Theor. Chem. Acc.* **2008**, *120*, 215–241.

(35) Patra, S. K.; Bera, J. K. Axial Interaction of the $[\text{Ru}_2(\text{CO})_4]^{2+}$ Core with the Aryl C-H Bond: Route to Cyclometalated Compounds Involving a Metal-Metal Bonded Diruthenium Unit. *Organometallics* **2006**, *25*, 6054–6060.

(36) Zhang, Y.; Santos, A. M.; Herdtweck, E.; Mink, J.; Kühn, F. E. Organonitrile Ligated Silver Complexes with Per-fluorinated Weakly Coordinating Anions and their Catalytic Application for Coupling reactions. *New J. Chem.* **2005**, *29*, 366–370.

(37) Marenich, A. V.; Cramer, C. J.; Truhlar, D. G. Universal Solvation Model Based on Solute Electron Density and on a Continuum Model of the Solvent Defined by the Bulk Dielectric Constant and Atomic Surface Tensions. *J. Phys. Chem. B* **2009**, *113*, 6378–6396.

- (38) (a) Ribeiro, R. F.; Marenich, A. V.; Cramer, C. J.; Truhlar, D. G. Use of Solution-Phase Vibrational Frequencies in Continuum Models for the Free Energy of Solvation. *J. Phys. Chem. B* **2011**, *115*, 14556–14562. (b) Funes-Ardoiz, I.; Paton, R. S. *GoodVibes v1.0.2*, 2016. DOI: [10.5281/zenodo.595246](https://doi.org/10.5281/zenodo.595246).
- (39) Frisch, M. J.; Trucks, G. W.; Schlegel, H. B.; Scuseria, G. E.; Robb, M. A.; Cheeseman, J. R.; Scalmani, G.; Barone, V.; Petersson, G. A.; Nakatsuji, H., et al. *Gaussian 16 Rev. A.03* 2016; Gaussian Inc.: Wallingford, CT, 2016.